BJR

Received: 24 August 2016 | Revised: 7 April 2017 | Accepted: 12 April 2017

https://doi.org/10.1259/bjr.20160710

Cite this article as:
Singh A, Kumar P, Chandrashekhara SH, Kumar A. Unravelling chloroma: review of imaging findings. *Br J Radiol* 2017; **90**: 20160710.

REVIEW ARTICLE

Unravelling chloroma: review of imaging findings

ANURADHA SINGH, MD, DNB, PAWAN KUMAR, MD, SHERAGARU HANUMANTHAPPA CHANDRASHEKHARA, MD, DNB and ATIN KUMAR, MD, DNB

Department of Radiodiagnosis, All India Institute of Medical Sciences, New Delhi, India

Address correspondence to: Dr Sheragaru Hanumanthappa Chandrashekhara
E-mail: *drchandruradioaiims@gmail.com*

ABSTRACT

Chloroma refers to the extramedullary proliferation of immature myeloid precursors occurring in a gamut of myeloproliferative and myelodysplastic conditions; acute myeloid leukaemia being the commonest. With non-specific clinical and imaging manifestations, it runs a high risk of misdiagnosis which may significantly affect the outcome of an otherwise treatable lesion. Also with these lesions heralding impending blast crises, awareness of the imaging findings becomes imperative. Imaging not only helps raise the suspicion but also guides further confirmation by demonstration of specific immunohistochemistry markers, ensuring timely institution of chemotherapy. In general, solid enhancing lesions in any haematological disorder could be chloromas, especially if multifocal with mass effect.

INTRODUCTION

Chloroma is a solid tumour composed of mass-like extramedullary proliferation of primitive cells of myeloid lineage causing effacement of the native tissue architecture. The first case of chloroma was observed by a British physician Burns[1] in 1811 in his observations on the surgical anatomy of the head and neck. Later in 1853, King[2] coined the term "chloroma" as the tumour was frequently of greenish hue due to the presence of myeloperoxidase enzyme. However, it was noted that up to one-third of these tumours can be white or grey. Hence, Rappaport[3] proposed the term granulocytic which is preferred and used interchangeably with chloroma.[4]

Chloroma may develop at any age. However, nearly 60% of cases are seen in children less than 15 years of age with no specific gender predilection. It is a rare manifestation of acute myeloid leukaemia (AML) with a reported incidence of 2.5–9%. Occasionally, it may be seen in other myeloproliferative or myelodysplastic conditions such as myeloid metaplasia, polycythemia vera, hypereosinophilic syndrome or essential thrombocytosis. Rare case reports suggest its occurrence in lymphoid leukaemia also.[5–8]

Chronology of occurrence of chloroma in myeloproliferative or myelodysplastic disorder is variable; accordingly, the following patterns may be seen (Audouin et al[9]):

(a) Concurrent with AML: commonest, manifesting at the time of initial presentation or any time during the active phase of AML.
(b) Relapse: presenting months to years later in AML remission, especially in recipients of Bone Marrow transplant. Chloroma developing during remission is considered as systemic disease despite normal blood counts and marrow findings.
(c) Precursor of blast phase transformation: in non-leukaemic myeloproliferative conditions, heralding blast crisis and subsequent AML transformation.
(d) Primary chloroma: a rare non-leukaemic form, occurring in otherwise healthy population in the absence of marrow abnormality. Primary chloroma precedes any haematological abnormality in nearly 35% of cases. Usually undergoes leukaemic transformation in months to years, average interval being 10 months.

Certain risk factors which increase the likelihood of developing chloroma in AML include M4 or M5 (French–American–British classification), myeloblasts-expressing specific T-cell markers CD13 and CD14, high peripheral total leukocyte count and certain chromosomal abnormalities t(8;21) or inv(16). On the contrary, chloroma in AML relapse may be due to certain biological peculiarities of leukaemic blasts cells such as molecular expression of markers responsible for increased tissue infiltration (CD87) and adhesion (CD56 and CD138). Frequent predilection of these lesions for certain sites propounds the hypothesis of suboptimal response to chemotherapy or graft-*vs*-leukaemia response.

Most common sites of chloroma are the bone and periosteum which is explained by the direct spread from the

adjoining infiltrated marrow. Other frequently involved sites are skin (leukaemia cutis), lymph nodes and orbit, although any site may be potentially affected. Chloroma has high propensity for recurrence with varying spatial and temporal distribution.[4–11]

DIAGNOSTIC MODALITIES

Chloroma usually remains asymptomatic (approximately 50%) or may have non-specific manifestations pertaining to the mass effect, organ dysfunction or pain at the involved site. Cross-sectional imaging is indispensable to delineate the sites and extent of involvement besides characterizing these lesions. The role of plain radiography is restricted to the evaluation of skeletal manifestations and preliminary evaluation of lung lesions or bowel obstruction. Ultrasound is expedient for assessing superficial structures such as skin, testis or during the follow-up of abdominal lesions.

Chloroma is a soft-tissue tumour which may be either circumscribed or diffusely infiltrating. CT findings are variable, which to some extent depend on the site of involvement. Usually craniospinal lesions are hyperdense on non-contrast CT (NCCT) and show intense homogeneous enhancement on contrast-enhanced CT (CECT). On the contrary, lesions in the abdominal viscera and orbit are frequently hypodense and mildly enhancing. MRI is helpful for evaluation of craniospinal and musculoskeletal involvement, especially in indeterminate cases. On MRI, it is iso-/hypointense on T_1 and mildly hyperintense on T_2 weighted images. MRI is also apt in follow-up imaging due to the lack of radiation concerns. Nuclear imaging such as fluorine-18 fludeoxyglucose (^{18}F-FDG) positron emission tomography (PET)/CT and gallium-67 is of value to look for multiplicity and response evaluation after chemotherapy. On ^{18}F-FDG-PET/CT and gallium-67 scans, chloroma shows avid uptake. ^{18}F-FDG-PET is imperative in radiotherapy planning. Despite all these imaging modalities, findings on sonography, CT, MRI or ^{18}F-FDG-PET remain generic, being indistinguishable from other malignancies and is frequently mistaken for lymphoma, a much commoner haematological malignancy.[8,9]

Diagnostic confirmation of chloroma is essentially established on immunohistochemistry (IHC) by demonstration of monoclonal antibodies against certain specific surface antigens. Most widely expressed markers are CD43, CD 68 and lysozyme. As per the World Health Organization classification (2008), specific cytochemical stains for diagnosing chloroma should include chloroacetate esterase, myeloperoxidase and non-specific esterase. A horde of other markers which may be expressed include CD4, CD33, CD34, CD56, CD117 or terminal deoxynucleotidyl transferase depending on the lineage and maturation of myeloid cells. There is a high likelihood of misdiagnosis on pathology, in as high as 47% of cases for the lack of specific IHC markers application, if chloroma is not suspected pre-emptively on imaging, especially in the non-leukaemic form.[8–11]

TREATMENT AND PROGNOSIS

Owing to its rarity, there is limited availability of data to establish the exact bearing of chloroma in the prognosis of

Table 1. Spectrum of systemic involvement in chloroma

Site	Pattern of involvement
CNS	Extra-axial: dura, periosteum, lepto-/pachymeninges (*leukaemic meningitis*)
	Intra-axial: nodules or masses (rare)
Spine	Epidural: intra-/extraspinal (commonest)
	Thecal sac/nerve root thickening
	Intramedullary (rare)
Neck	Involvement of any neck space
	Transcompartmental spread ±
Orbit	Extraconal (common)
	Bony orbit/periosteum
	Extra-ocular muscles
	Optic nerve
	Intraconal
	Intra-ocular (sclera/choroid/retina)
Thorax	Mediastinum
	Any compartment may be involved
	Trans-compartmental spread ±
	Lung
	Alveolar involvement: nodules, masses
	Interstitial involvement: septal thickening
	Pleura and pericardium
	Nodules
	Effusion
Hepatobiliary	Discrete masses (solitary/multiple)
	Peribiliary chloroma
Gastrointestinal	Nodule, polyp, ulcer, diffuse segmental thickening of the involved bowel
	Peritoneal, omental deposits ±
	Mesenteric lymphadenopathy/ascites
Genitourinary tract	MC site in
	Male: testis and adnexa
	Female: ovary
Breast	Solitary or multiple masses
Muscles	Primary or secondary to contiguous spread from the adjacent bone
	MC site: pelvic muscles
Skin, lymph node	Skin: papulonodular eruptions (leukaemia cutis)
	Lymph node: solitary or multiple lymphadenopathy; may be discrete or conglomerate
Bone	MC site of involvement
	Lytic or mixed lytic–sclerotic lesion

CNS, central nervous system; MC, most common.

leukaemia or other myeloproliferative conditions. In AML, prognosis largely remains unchanged; however, studies do suggest refractoriness to therapy and increased likelihood of relapse. On the contrary, primary myeloid sarcoma or chloroma in AML remission is labelled as systemic disease and treated on the lines of leukaemia even with normal peripheral leukocyte counts or Bone Marrow (BM). Similarly, chloroma in various other myeloproliferative and myelodysplastic conditions suggests leukaemic transformation and warrants systemic anti-leukaemic chemotherapy. Localized treatment such as surgery or radiotherapy is highly effective in relieving compressive symptoms particularly in spinal chloroma and may provide immediate survival benefits in some cases; however, overall survival or prognosis remains unaffected and is determined by the systemic disease.[12,13]

On an average, the median survival after the diagnosis of chloroma is 7.5 months. Prognosis is unfazed by the age, gender or the underlying myeloproliferative/myelodysplastic condition. By and large, prognosis is independent of the site of involvement; however, lesions at uncommon sites may prove detrimental primarily due to delayed recognition, although the lesions may not necessarily be more aggressive than their counterparts elsewhere.[12–14]

A recent surge in the incidence of chloroma is likely due to prolonged longevity in leukaemia consequent upon the availability of newer treatment options (*e.g.* allogenic Bone Marrow transplantation, repeated donor lymphocyte infusion, second transplantation). Nevertheless, diagnosing chloroma, especially the non-leukaemic form, is quite challenging and is essentially a holistic approach involving clinical, laboratory and imaging findings. Radiologists are often the standard bearer in arriving at the diagnosis by raising its suspicion on imaging which guides the haematopathologist to execute flow cytometry, IHC and immunophenotyping accordingly. For the impact on prognosis and overall survival, radiologists should be aware of the possible imaging manifestations, potential sites of involvement particularly in known haematological malignancy to alarm its suspicion, facilitating early diagnosis which may alter the management and halt further disease progression. Few series have also reported a lower rate of leukaemic transformation if primary MS is recognized and treated timely. Despite aggressive and extensive involvement, these lesions are highly responsive to induction chemotherapy; furthermore, stressing the need of timely recognition.[7]

A systemic review of imaging findings in chloroma is presented here (Table 1) along with site-specific common differential considerations.

Figure 1. Central nervous system chloroma: a 12-year-old male of acute myeloid leukaemia presented with scalp swelling, headache and seizures. Contrast-enhanced CT (CECT) head (a–c) revealed multiple intensely enhancing extradural masses (arrows); left sigmoid sinus lesion had additional transcalvarial spread with scalp infiltration. Another similar mass was present in midline (c) with sagittal sinus infiltration resulting in thrombosis. All these lesions were causing calvarial erosion (arrow in d). Follow-up CECT (e, f) 10 days after induction chemotherapy showed significant reduction in the size of these masses (arrows).

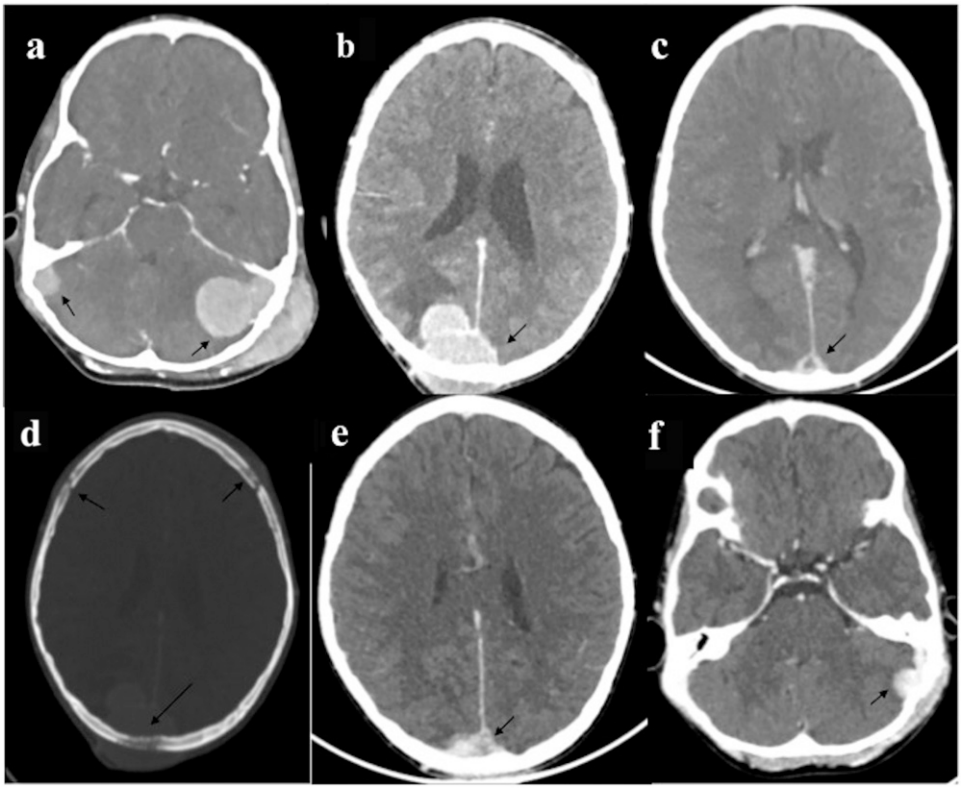

Central nervous system

Intracranial

Central nervous system (CNS) chloroma is postulated to originate secondary to the calvarial marrow infiltration with subsequent transgression of leukaemic infiltrates through the haversian canal and further extramedullary proliferation in the subperiosteum. This accounts for the frequent epidural location of these lesions, in concordance with the calvarial proximity. Subarachnoid space involvement is believed to result from the perivenular arachnoid spread of leukaemic infiltrates along the dural or subarachnoid veins. Intracranial chloroma is further categorized into intra- or extra-axial depending upon its location.[5,7,8,15–19]

Extra-axial

- *Epidural/subdural deposits* (Figure 1) may be discrete or contiguous and usually propogate along the cerebral venous sinus with propensity for causing venous infarction.
- *Meningeal involvement* (Figure 2): plaque-like involvement of lepto- or pachymeninges also called carcinomatosis or leukaemic meningitis. Ependymal spread may lead to intraventricular deposits.

Intra-axial Intra-axial chloroma is extremely rare (Figure 3) and is usually due to parenchymal invasion by the extra-axial deposits following breach of the pia–glial membrane. Rarely, it may be primary intra-axial in the form of circumscribed masses with occasional intralesional haemorrhage and disproportionate perilesional oedema causing mass effect. There is no specific lobar predilection.

On NCCT, cranial chloroma is usually hyperdense solid masses of soft-tissue attenuation which is attributed to the compact cellular packing. On MRI, these lesions are usually iso-/hypointense to grey matter on T_1 and is likely due the presence of myeloperoxidase enzyme. On T_2 weighted imaging (T2WI), lesions are mildly hyperintense. Usually, these lesions show intense homogeneous enhancement. Rarely, ring enhancement may be encountered especially in larger lesions or during treatment which is due to the central necrosis. Ancillary

Figure 2. Central nervous system chloroma: a 2-year-old female presented with diffuse scalp swelling and vomiting. (a) Contrast-enhanced CT (CECT) of the head showed plaque-like extradural enhancing mass involving the anterior and middle cranial fossa including bilateral orbits with (b) marrow infiltration resulting in spiculated periosteal reaction. Initially, thought to be neuroblastoma for the age and imaging appearance, bone marrow and biopsy confirmed acute myeloid leukaemia. (c, d) A 5-year-old male with leukaemia developed meningismus. CECT of the head revealed enhancing deposits in leptomeninges and left external capsule. Lumbar puncture was sterile with the presence of blast cells suggestive of leukaemic meningitis.

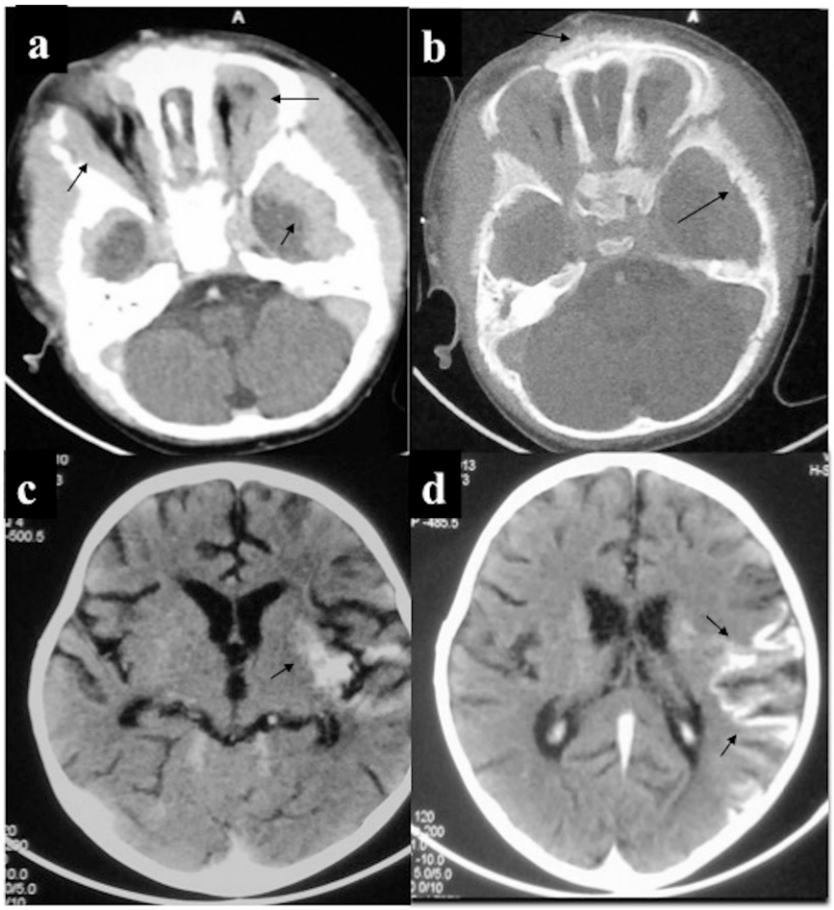

Figure 3. Intra-axial central nervous system chloroma (a–d): a 5-year-old male with acute myeloid leukaemia presented with features of raised intracranial tension and generalized tonic–clonic seizures. MRI showed multiple circumscribed lesions of intermediate T_2 signal intensity (a, b) involving bilateral cerebral hemispheres including basal ganglia with perilesional oedema (PLE). On contrast-enhanced MRI, these lesions showed solid or ring enhancement. Additionally, there was patchy leptomeningeal enhancement (arrows in c). (e, f) CECT of a 26-year-old leukaemic patient performed for headache showed lenticular extra-axial mass with peripheral enhancement and focal bony erosion in the right frontal lobe. Medial border of this lesion was irregular with nodular component showing parenchymal invasion and PLE.

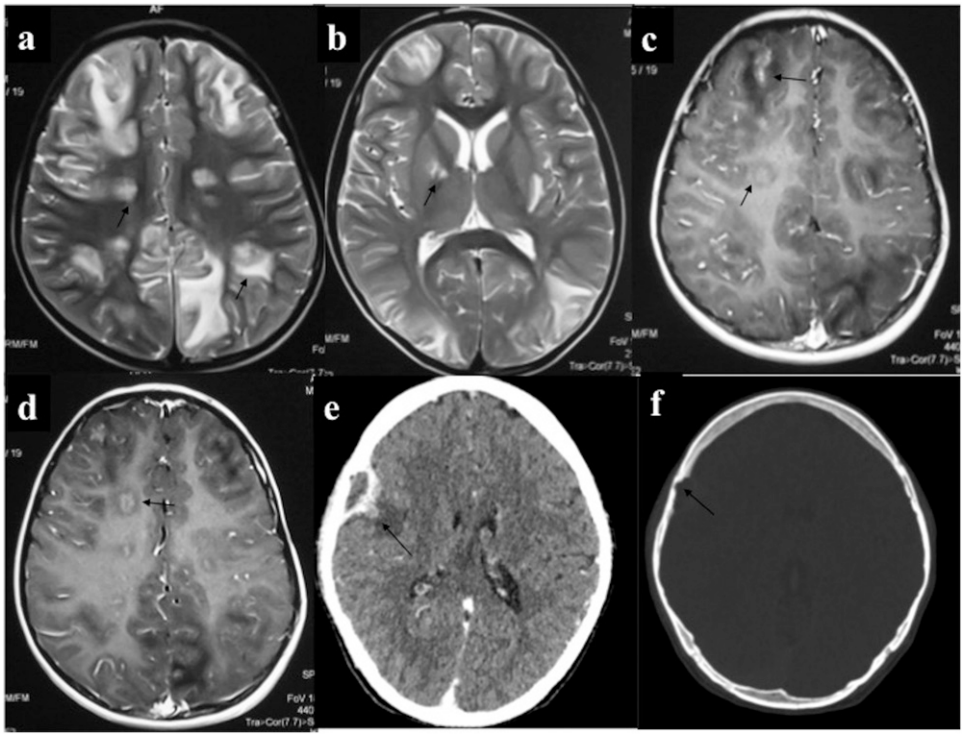

features may include bone erosion and venous sinus thrombosis. Although tissue sampling is required for diagnostic confirmation, which may be obviated in a known myeloproliferative disorder with these classical imaging findings, and is reserved only for indeterminate cases.

A rare but essential contemplation in CNS chloroma is the subdural deposits with its clinical and imaging findings being strikingly similar to the subdural haematoma (SDH); latter being relatively common due to coagulopathy in haematological malignancies. Furthermore, concomitant occurrence of subdural deposits with SDH fuels the complexity which needs to be distinguished for their antipodal management (Figure 4). SDH requires surgical drainage, whereas subdural chloroma is managed conservatively with systemic chemotherapy and adjunctive radiotherapy; surgery is rarely required in CNS chloroma to relieve mass effect. Contrast study [CECT/contrast-enhanced MRI (CEMRI)] is invaluable in this distinction as subdural deposits are intensely enhancing as opposed to SDH which lacks enhancement.[20,21]

Spine

Similar to cranial chloroma, spinal involvement is usually secondary to the leukaemic marrow infiltration with further transgression of myeloid cells through the haversian canal in the extra-osseous location. Accordingly, chloroma of the spine is usually extramedullary in location, commonly epidural and is either within the spinal canal or may track along the nerve roots in the paraspinal location (Figures 5–7). Pre-/paravertebral chloroma may also be due to the spread from retroperitoneal lymphadenopathy. Intramedullary chloroma of the cord is extremely rare (Figure 8).

Spinal chloroma frequently leads to compressive myelopathy/neuronopathy regardless of the site of involvement. MRI is the modality of choice for evaluation of spinal deposits. It presents as multiple extramedullary masses which may be either contiguous or discrete involving different vertebral levels. These deposits are usually isointense on T_1, intermediate on T_2 and show homogeneous enhancement. Furthermore, there is diffuse leukaemic infiltration of the vertebral marrow. Combined intra-extraspinal form of chloroma may mimic nerve sheath tumour on imaging; however, lack of profound T_2 hyperintensity with no secondary bony changes (destruction or remodelling) favours chloroma. Accurate and timely diagnosis of chloroma is imperative as local control of the disease with focused radiotherapy or adjuvant chemotherapy helps in relieving cord compression besides obviating unnecessary surgery. Such directed therapies improve the quality of life with immediate survival benefits, although overall prognosis remains bleak.[5,7–11,22–24]

Figure 4. Extra-axial chloroma with subdural haematoma (SDH): a 54-year-old male having Chronic Myeloid Leukemia with altered sensorium (a) non-contrast CT of the head revealed SDH along bilateral cerebral convexity (straight arrows). Additionally, multiple nodular hyperdense masses (curved arrows) were discernible peripheral to the SDH. (b–f) MRI performed for further characterization demonstrated subacute SDH (arrow in b) and multiple extradural nodules along bilateral cerebral convexity and along falx cerebri which were isointense on T_1 (curved arrows in c) and showed intense enhancement (straight arrows in d–f). Diffuse plaque-like pachymeningeal enhancement (curved arrows d–f) was also present. Subsequently performed bone marrow examination revealed blast phase transformation.

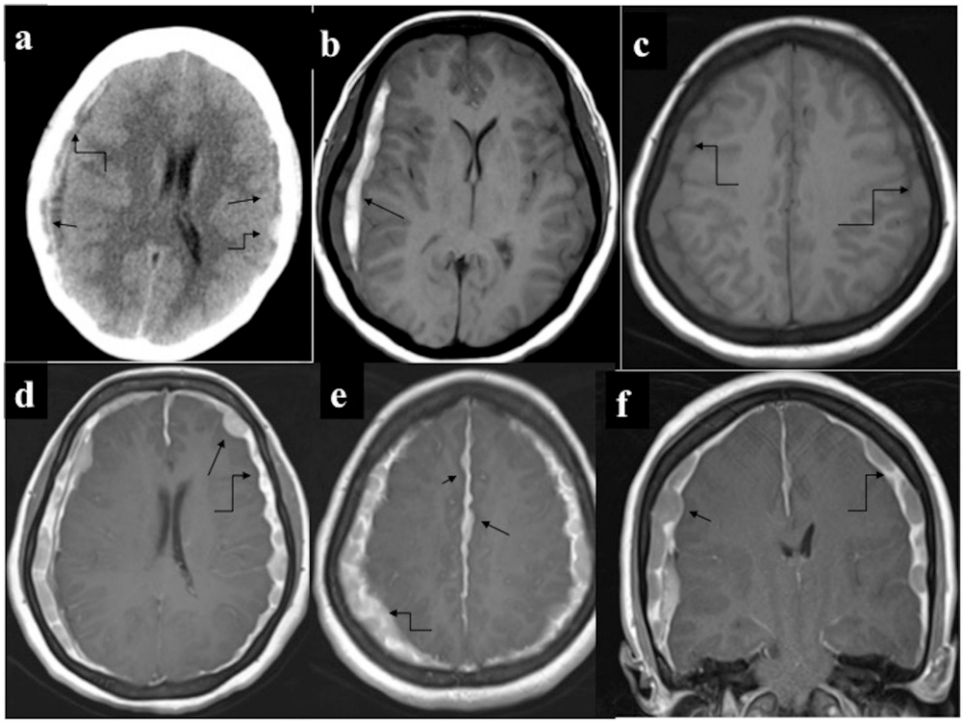

Head and neck

Orbit is the commonest site to be involved in the head and neck region. Prevalence of orbital chloroma is higher in children than in adults. Orbital involvement may be uni- or bilateral and may result in proptosis, venous congestion or blindness. Virtually, any structure of the orbit whether intra- or extraconal may be affected (Figure 9); the commonest site being the subperiosteum of the roof of the orbit. Rarely, optic nerve deposits may occur especially during the leukaemic relapse as the retrobulbar optic nerve is a sanctuary site for the leukaemic infiltrates due to suboptimal penetration of the chemotherapy drugs.

On NCCT, orbital chloroma is usually iso-/hypodense with mild homogeneous enhancement. It molds along the bony contour without causing its destruction; however, the medial orbital wall remains an exception through which it contiguously extends into the paranasal sinus. Nonetheless, with extensive disease, orbital chloroma may spread to the paranasal sinuses and *vice versa* with resultant cortical destruction and periosteal reaction (spiculated or "hair on end").

Intra-ocular chloroma may involve various coats of the eyeball such as the sclera, uvea or retina. On CT, due to poor contrast resolution, differentiation of these deposits from the adjoining normal tissue may be difficult which is essential if surgical debulking is planned. MRI is of paramount utility in such cases, especially to delineate scleral involvement for the relative iso-/hyperintense signal intensity of these lesions as against the hypointense sclera.

Paranasal sinus involvement may vary from mucoperiosteal thickening, focal circumscribed masses or opacification of the entire sinus with bone destruction in advanced stages. Other sites to be involved in the head and neck region include mucosa of the lips, gingiva, nose and skin (Figure 10). Cervical involvement frequently manifests as lymphadenopathy which may be discrete or conglomerate. Occasionally, there may be infiltrating mass-like deposit lacking compartmental localization. Owing to the superficial location, these deposits are usually detected early. However, if undiagnosed, it may further spread to adjacent structures such the orbit or paranasal sinuses. Orbital and neck chloroma are highly liable to intracranial extension through the skull base foramina.[5,7,11,25,26]

Thorax

Intrathoracic chloroma is an infrequent site, and of the various potential sites, mediastinum is the commonest to be affected (Figures 11 and 12).

Mediastinum

Mediastinal chloroma can be in the form of discrete masses or more commonly as diffusely infiltrating soft tissue which may

Figure 5. Various patterns of spinal myeloid sarcoma: (a) paraspinal deposits: non-contrast CT chest showed lobulated right paraspinal deposits (arrow) with bilateral mild pleural effusion. (b, c) Combined extra-intraspinal forms: axial and sagittal oblique contrast-enhanced CT: infiltrating enhancing epidural deposit (arrows) in the lower cervical spine with extension along the left neural foramina into paraspinal location. (d–f) Epidural deposit: MRI of the spine of a 32-year-old patient in acute myeloid leukaemia remission performed in view of backache revealed well-defined soft-tissue deposit in the posterior epidural space in the upper thoracic region (arrows) which was isointense on both T_1 (d) and T_2 (e) weighted imaging, with intense homogeneous enhancement. No marrow or signal alteration in the cord present.

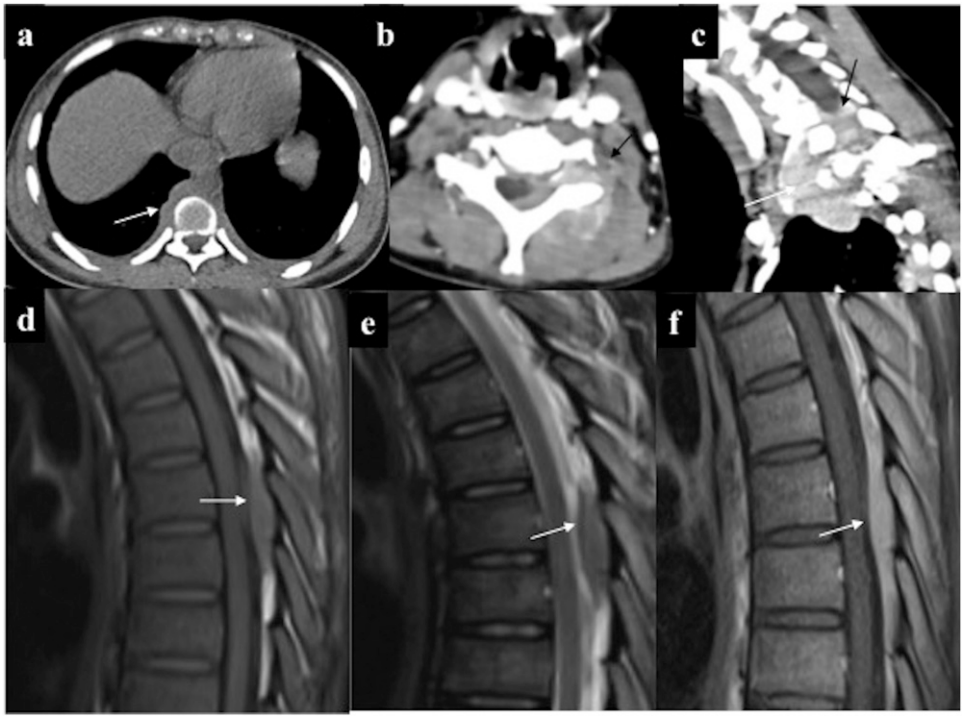

have transcompartmental involvement and is frequently mistaken for lymphoma on imaging. Symptoms result from compression of various mediastinal structures. Cardiac chloroma is an extremely rare entity which may involve any cardiac chamber or valve.[5,7,9]

Lung

Lung chloroma is extremely rare and may involve interstitium or alveoli. The various morphological patterns include consolidation, nodules, masses (solitary or multiple) or interstitial thickening. Lung involvement usually manifests as interstitial thickening which is indistinguishable from interstitial pneumonitis or fluid overload. Consolidation and masses are extremely rare. In the early stages, air bronchogram may be present; however, in advanced disease, large masses may compress the lung parenchyma with frequent pleural and mediastinal involvement.

Nodules may undergo cavitation with surrounding ground-glass attenuation giving rise to the classical "reversed halo sign" on CT, making it virtually indistinguishable from the fungal infection. Although exceptional, radiologists should be aware of the possibility of chloroma and offer tissue sampling, especially in the wake of non-resolving or progressive disease, despite antifungal treatment. Interstitial involvement leads to septal thickening which may be smooth or nodular. Lung chloroma, in general, has dismal prognosis despite intensive chemotherapy, perhaps due to its late recognition.[5,7,27,28]

Pleura and pericardium

Pleural or pericardial deposits may be nodular or plaque-like and usually result in concomitant effusion.[5,7]

Abdomen

Hepatobiliary

Myeloid cells may infiltrate hepatic sinusoids or peribiliary venous plexus resulting in circumscribed lesions or periportal infiltration also referred as "peribiliary chloroma" (Figure 13). On CT, these nodules are usually hypodense with mild or no contrast enhancement. These nodules mimic infection/abscess or more commonly lymphoma. Unlike lymphoma which lacks mass effect, myeloid deposits commonly lead to obstructive jaundice. Obstructive jaundice resulting from peribiliary chloroma usually proves detrimental for its frequent ascription to cholangitis or adverse effect of chemotherapy.

Although pancreatic chloroma is extremely rare, pancreatic head deposit may lead to obstructive jaundice. Similar to hepatic deposits, these lesions are iso- or hypodense on CT with mild enhancement, making it indistinguishable from pancreatic adenocarcinoma or lymphoma on imaging.[6,11,15]

Figure 6. (a, b) Epidural chloroma causing cord compression: mildly T_2 hyperintense (a) enhancing (b) epidural deposit (straight arrows) in the upper thoracic region which is encasing and causing signal alteration in the cord (curved arrows). Note leukaemic marrow infiltration. (c, d) Paraspinal deposits: few homogeneously enhancing paraspinal deposits with neural foraminal extension of the lesions in the left upper thoracic region resulting in a "dumb-bell shape" configuration, (better appreciated in sagittal oblique; d) making it indistinguishable from nerve sheath tumour on imaging.

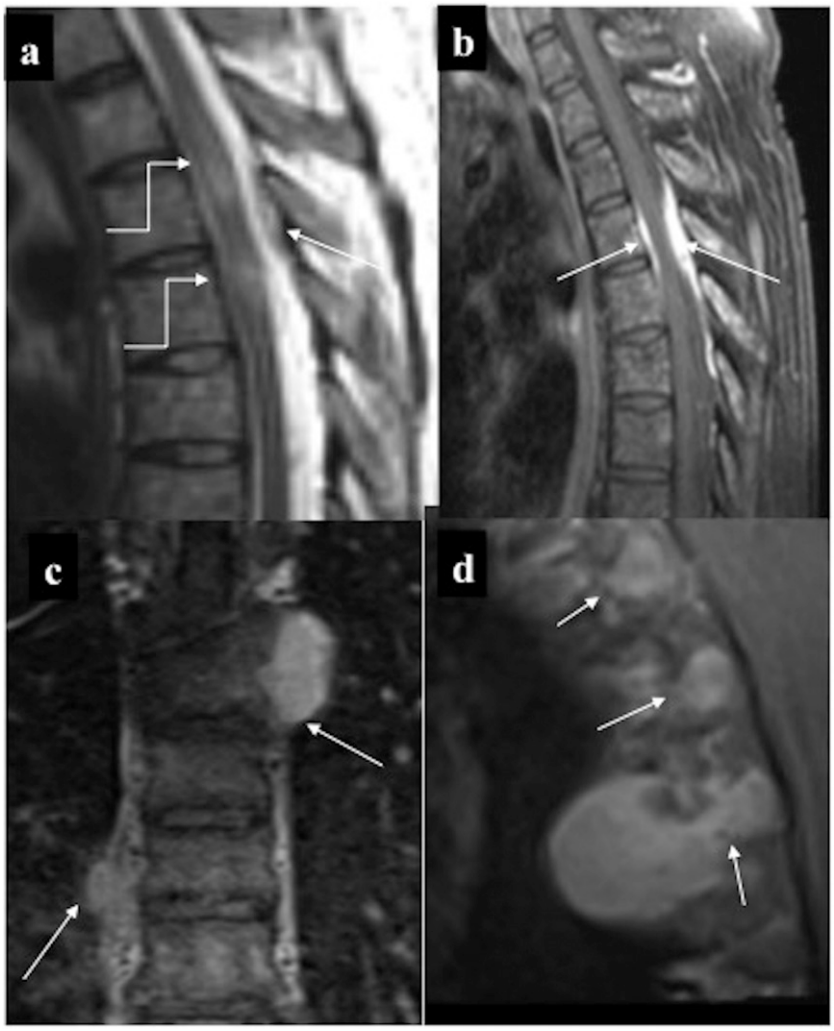

Gastrointestinal tract (bowel, omentum and peritoneum)

Gastrointestinal tract (GIT) chloroma is extremely rare and is believed to stem from haematopoietic cell rests. It frequently leads to calamitous manifestations such as bowel necrosis, obstruction, perforation or torrential haemorrhage, unlike their counterparts elsewhere. Analogous to bowel lymphoma, the small intestine is the commonest site to be involved

Figure 7. Intraspinal chloroma. (a) Enhancing epidural deposit (straight arrow) causing cord compression along with thickened and enhancing intradural nerve (curved arrow) root with left costovertebral deposits (solid arrow). (b) Intradural solid soft tissue with central necrosis (arrow) causing eccentric compression of thecal sac. (c) Chloroma deposits causing thickening and enhancement of the cauda equine nerve roots along with their clumping resulting in "pseudotethered cord" (arrows). Dural enhancement was also present.

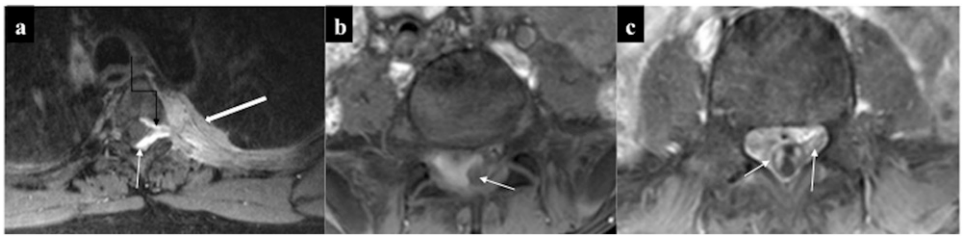

Figure 8. (a–e) Intramedullary chloroma: a 6-year-old leukaemic patient with sudden onset quadriplegia. (a–e) MRI showed mild expansion with cerebrospinal fluid (CSF) effacement of the cord spanning almost two vertebral segments in the upper thoracic region. The involved segment was T_1 isointense, mildly T_2 hyperintense (b, c) and demonstrated intense homogeneous enhancement (d, e). (f) Spinal leptomeningeal involvement: contrast-enhanced MRI of the spine of a different leukaemic patient showed continuous leptomeningeal enhancement along the ventral surface of cord (arrows) raising the possibility of leptomeningeal involvement which was later confirmed on CSF analysis.

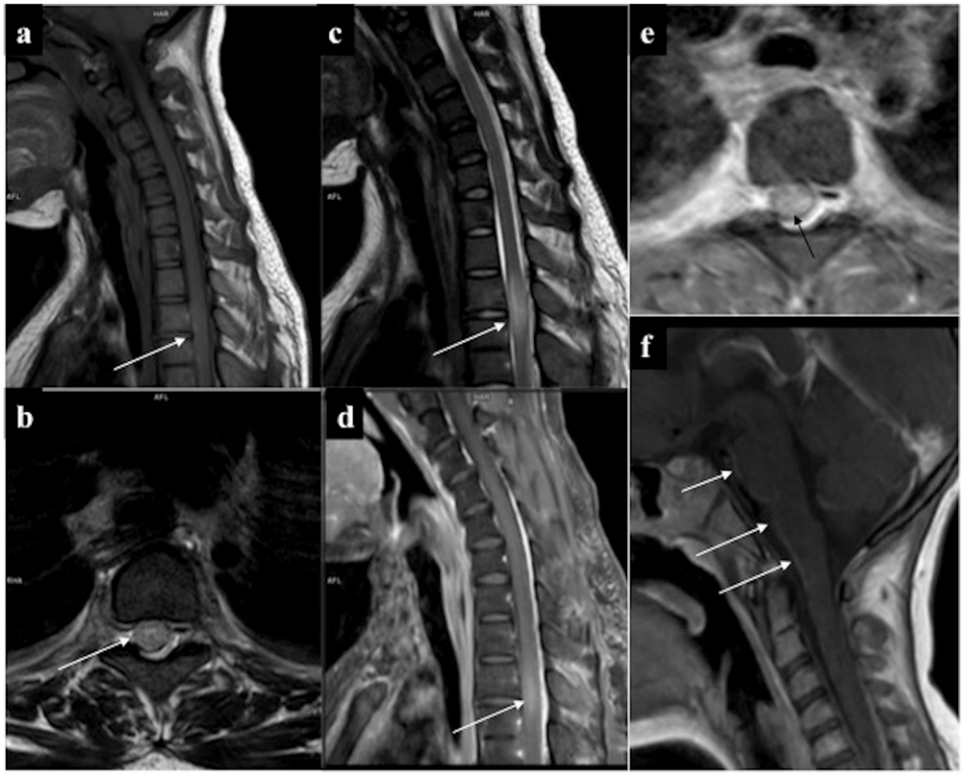

(Figures 14 and 15). Isolated involvement of colon or rectum is even rarer and is usually secondary to the peritoneal involvement. Morphologically, different patterns of GIT chloroma include nodules (solitary/multiple), polyps, ulceration or segmental mural thickening resembling a stricture. Bowel chloroma has a high tendency for extraluminal spread into the mesentery or omentum. In advanced cases, there may be peritoneal involvement which

Figure 9. Orbital chloroma (different patients) (a) Bilateral circumscribed enhancing extraconal deposits superolaterally (arrows). (b, c) Diffusely infiltrating hypoenhancing deposit involving left orbit both intra- and extraconally resulting in thickening of recti and the optic nerve (curved arrows). Note subconjunctival deposit (straight arrows) and mild left proptosis. (d, e) Bilateral conjunctival chloroma (straight arrows) with abnormally deep left anterior chamber (curved arrows), better appreciated in sagittal oblique (e). Ultrasound (not shown) revealed deposits. (f) Case of right orbital chloroma with contiguous extension to the cavernous sinus (arrows).

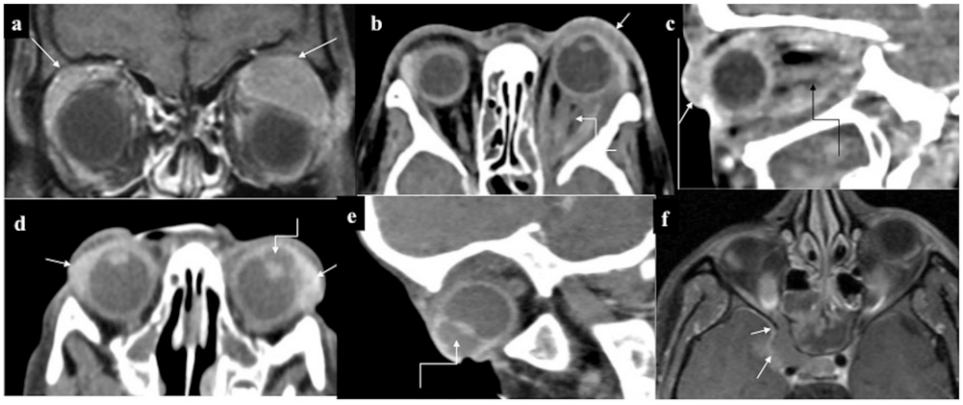

Figure 10. Involvement of various neck spaces (different patients). (a) Intensely enhancing deposit in the left perivertebral space, (b) right parapharyngeal, nasopharynx (curved arrow) and the left perivertebral region (c). Large necrotic mass in the left posterior cervical space, treatment naïve (d). Heterogeneously enhancing deposits in the right parotid and right perivertebral space (e), deposits in the left masticator, infratemporal fossa, parapharyngeal space (f), multiple lobulated deposits in left submandibular and bilateral anterior triangle (g). Lobulated infiltrating mass in the vestibular mucosa with involvement of the upper lip (h) and chloroma deposit in the left nasal cavity (i, j). Fluorine-18 fludeoxyglucose (^{18}F-FDG) positron emission tomography/CT of different patients showing multiple bilateral cervical deposits with intense ^{18}F-FDG avidity.

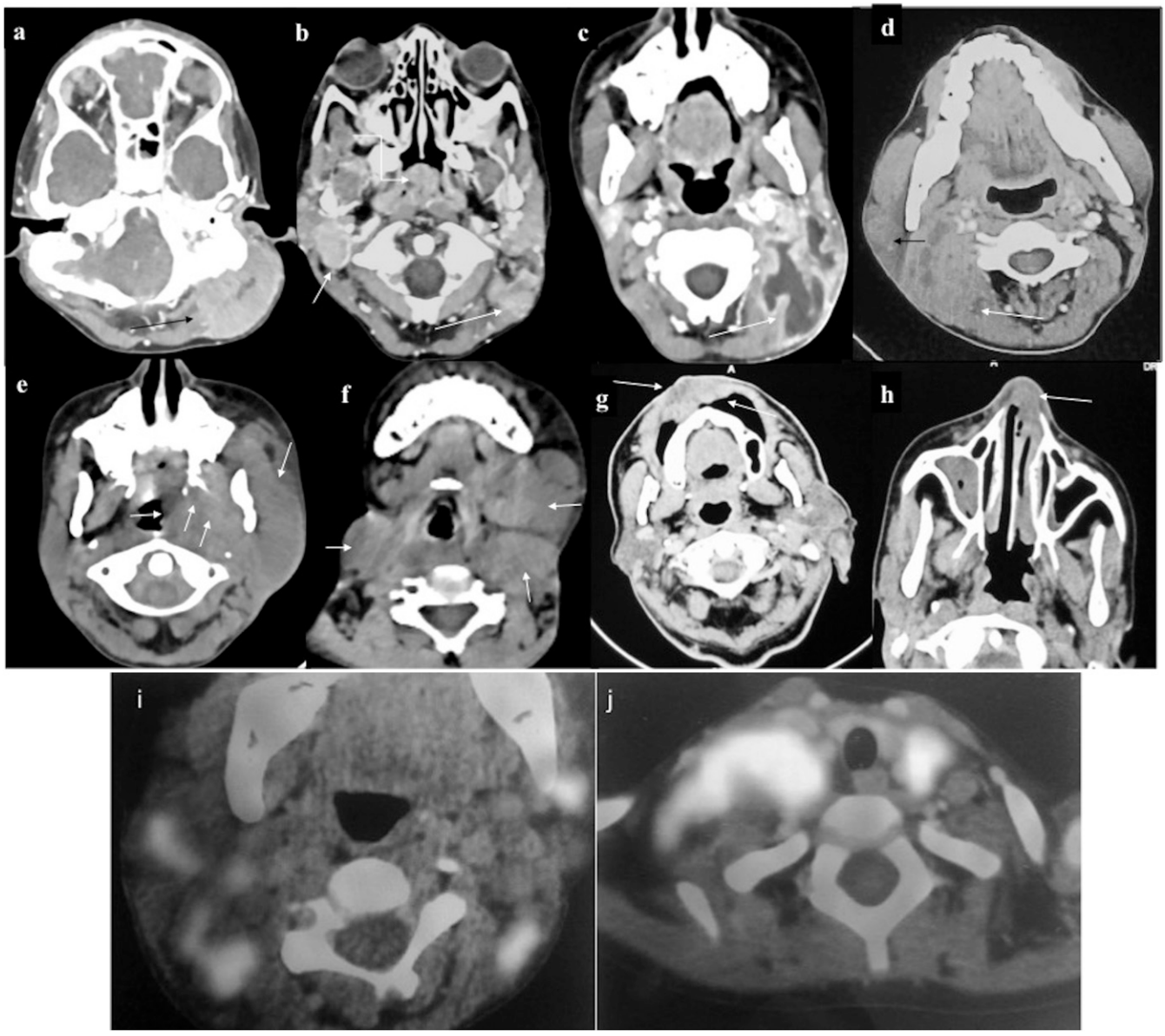

resembles peritoneal carcinomatosis or lymphomatosis on imaging.

Of the abdominal viscera, the spleen is the commonest site to be involved followed by the liver. However, whether or not splenic involvement is considered extramedullary, relapse remains controversial as many authors propound the spleen to be a medullary organ.[5,7–11,15]

Genitourinary tract

Although rare, any part of the genitourinary tract may be involved. Of the reproductive and urinary tract, the former is more commonly involved.

Urinary tract

Similar to GIT, chloroma of the genitourinary tract is also postulated to originate from the haematopoietic cell rests.

Figure 11. Intrathoracic chloroma: a 43-year-old male Known case of Chronic Myeloid Leukemia developed haemoptysis with right lower zone consolidation on chest radiograph (not shown). Contrast-enhanced CT (a–c) showed mass-like consolidation in the right lower lobe (RLL) (straight arrows) with mild pleural effusion (curved arrow in a) and mediastinal lymphadenopathy (curved arrow in c) raising the possibility of infective aetiology. Despite antibiotics, owing to persistent symptoms, repeat non-contrast CT (d–f) was performed 20 days later which showed progression in consolidation of RLL with appearance of air bronchogram (arrow in d) and cavitation (arrow in e), as well as increase in pleural effusion. Additionally, patchy consolidation developed in Right middle lobe (arrow in f). Biopsy revealed myeloid sarcoma; however, despite initiation of treatment, the patient succumbed to his illness after a month.

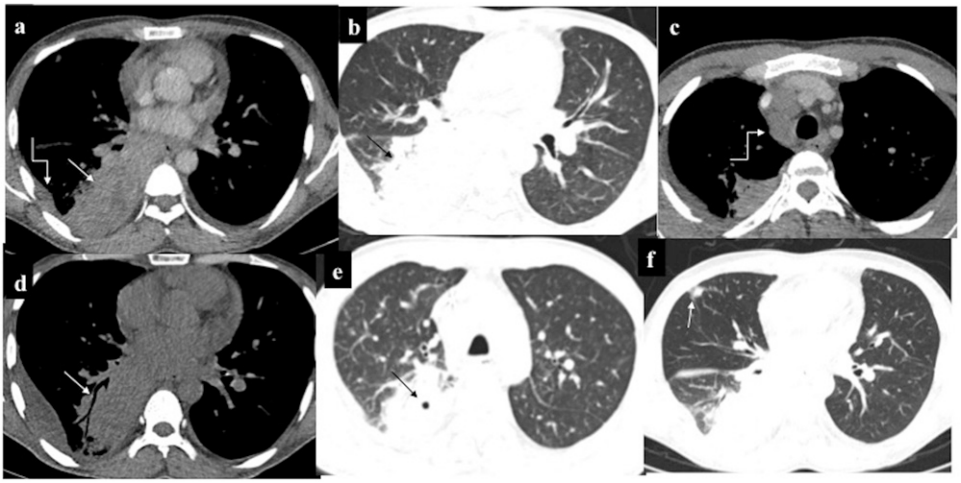

According to the site of involvement, urinary tract chloroma may manifest with abdominal pain, haematuria or hydronephrosis.

Ante-mortem diagnosis of non-leukaemic renal chloroma is extremely unusual. Renal involvement is usually diffusely infiltrating resulting in nephromegaly with variable

Figure 12. Intrathoracic chloroma (different patients): (a, b) parenchymal deposit in Left lower lobe with adjacent pleural and paraspinal muscle infiltration (arrow in a). On lung window, tiny eccentric cavitation (arrow in b) and perilesional ground-glass attenuation can be appreciated (c, d). Combined alveolar and interstitial pattern: patchy consolidation with surrounding ground-glass attenuation in Right middle lobe and right lower lobe with interlobular septal thickening and ipsilateral pleural effusion (e, f). A patient with acute myeloid leukaemia on chemotherapy who complained of chest pain and breathlessness. Chest radiograph revealed opaque right hemithorax with contralateral cardiomediastinal shift suggesting likely pleural effusion for which intercostal drainage tube was placed. However, owing to persistent symptoms, contrast-enhanced CT was performed which revealed heterogeneously enhancing infiltrating mass in the right lung causing abrupt cut-off of the right mainstem bronchus (best appreciated in minimum intensity projection image), (h) with mediastinal invasion (curved arrows in e, f) and pleural and pericardial effusion. Biopsy was consistent with myeloid sarcoma. Following chemotherapy and radiotherapy, there was complete resolution of the mass.

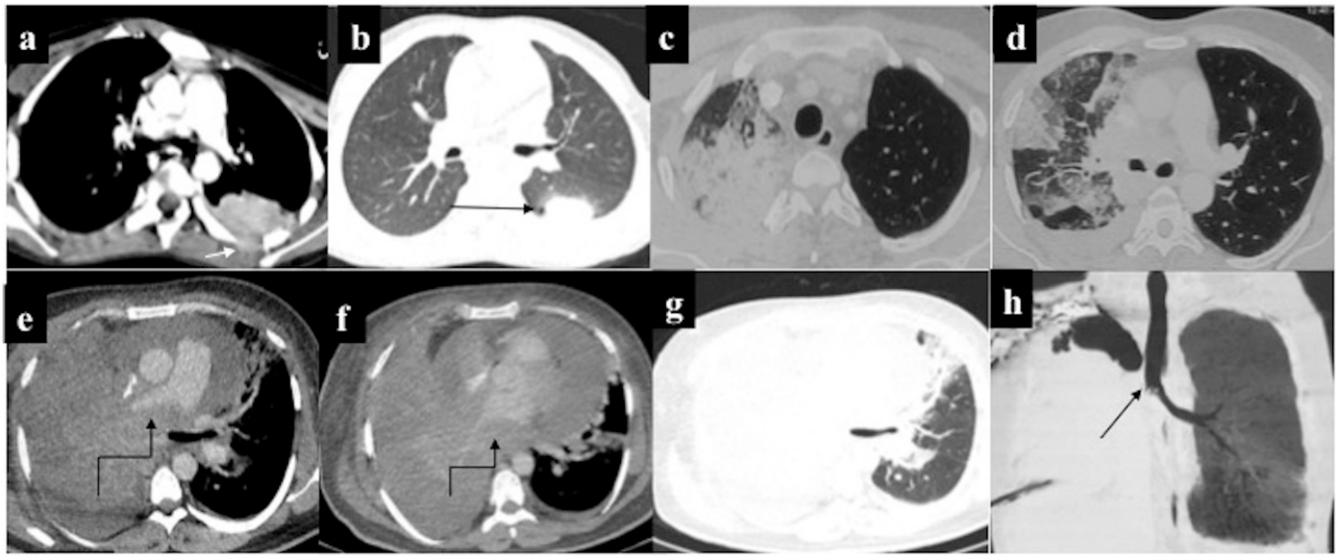

Figure 13. Hepatobiliary chloroma: contrast-enhanced CT of the abdomen of a 21-year-old male on chemotherapy for acute myeloid leukaemia who developed obstructive jaundice, revealing (a) mild hepatomegaly with multiple discrete hypovascular masses (arrow) involving both the lobes of the liver. (b–d) Additionally, an ill-defined hypovascular mass was present in the pancreatic head region causing mild dilatation of upstream Main pancreatic duct. A similar mass was seen involving the right adrenal gland (arrows in c, d). Biopsy of the hepatic mass was consistent with chloroma. Despite ongoing chemotherapy, the patient died 2 weeks later.

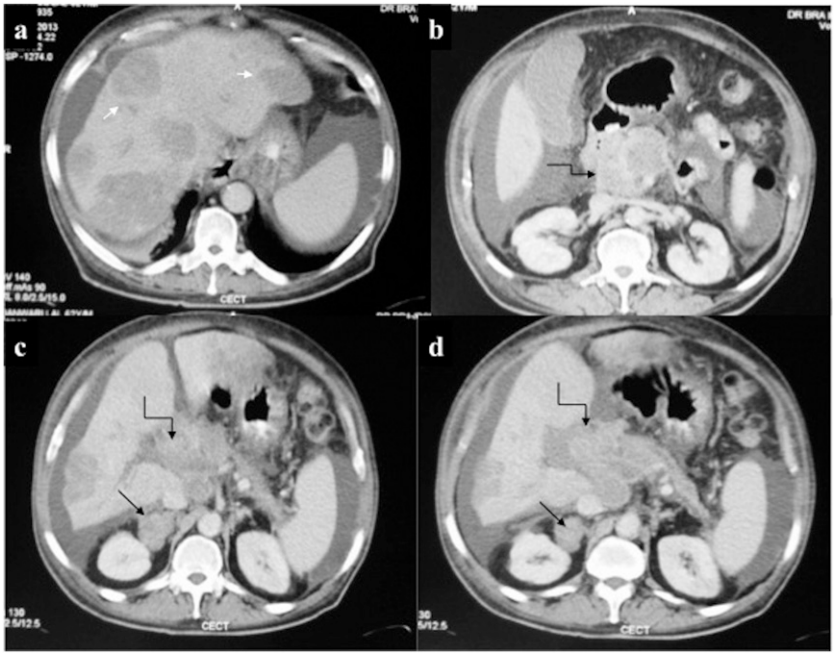

extension to the perinephric space. Pelvicalyceal or ureteric involvement may be suggested by plaque-like mucosal thickening which is indistinguishable from transitional cell carcinoma. Urinary bladder chloroma usually results in mural thickening which may be focal or diffuse.

Figure 14. Contrast-enhanced CT of the abdomen of a 41-year-old male with no prior significant medical history presented with intestinal obstruction for which exploratory laparotomy was performed which revealed a mass at the ileocaecal junction, initially diagnosed as T-cell lymphoma. Subsequently, abdominal CT was performed for staging which revealed: (a) long segment circumferential thickening of the jejunum (arrows) with proximal dilatation. (b) A distinct hypovascular mass was present at the root of mesentery (arrow) with vessel coursing through it. Bone marrow examination, however, was consistent with acute myeloid leukaemia following which biopsy of the mesenteric mass was repeated percutaneously. Immunohistochemistry confirmed it to be chloroma. (c, d) Follow-up scans obtained after 2 months of chemotherapy revealed mild residual thickening in the jejunum (arrows) with resolution of mesenteric mass.

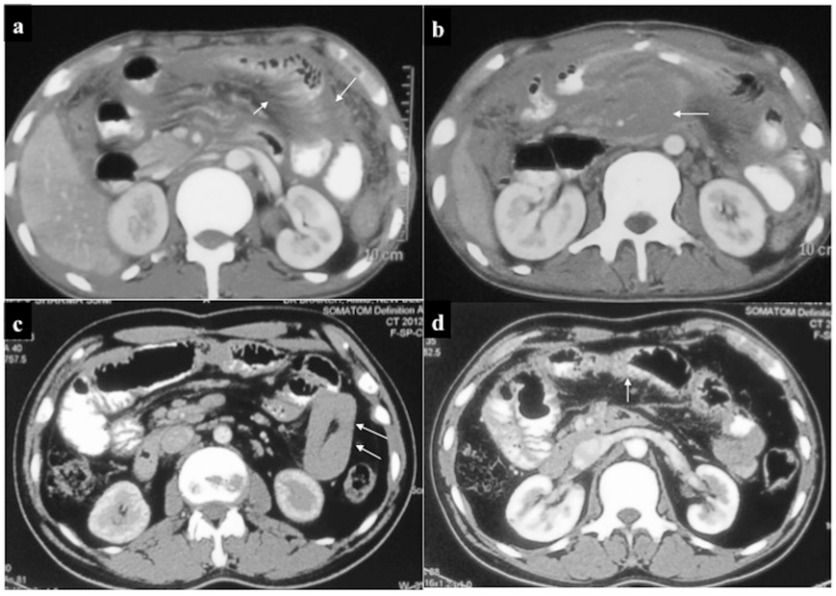

Figure 15. Pre-sacral chloroma with rectal infiltration. (a, b) Contrast-enhanced CT and contrast-enhanced MRI images of a 5-year-old male with leukaemia with constipation showing large enhancing pre-sacral deposit (arrows) which is anteriorly displacing and infiltrating the rectum, no bone erosion (c) Follow-up MRI after 30 days showed near-complete resolution of the deposit.

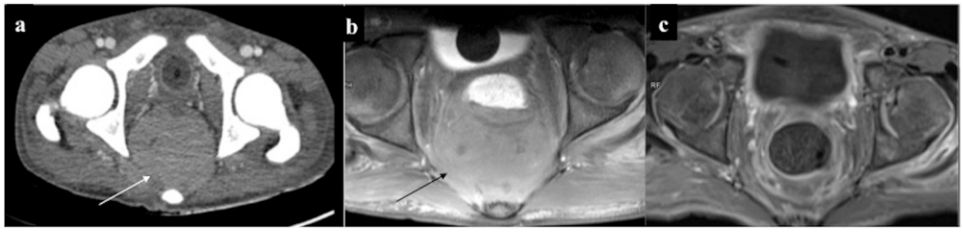

Figure 16. (a, b) Case of treated acute myeloid leukaemia with left testicular swelling. Ultrasonography of the scrotum revealed normal right testis (a). However, the left testis was mildly bulky and diffusely hypoechoic suggestive of extramedullary relapse. The epididymis was not involved.

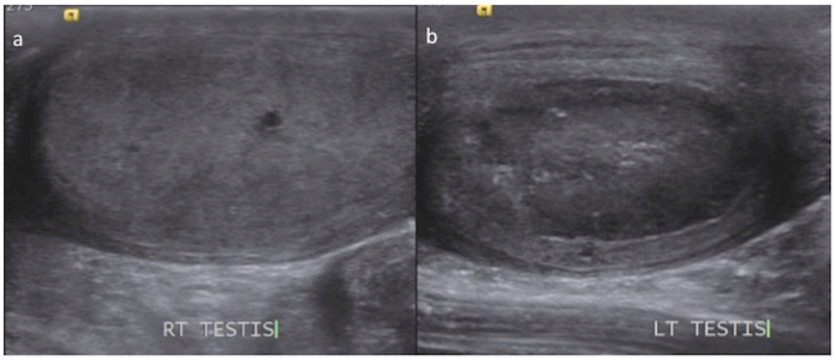

Reproductive tract

In females, chloroma commonly involves the ovary. Ovarian chloroma may have different morphological patterns varying from solid and homogeneously enhancing to solid–cystic or, less commonly, multiseptated. Although less common, there may be involvement of the uterus and cervix. Vagina and vulval deposits are extremely rare.

In the male reproductive tract, the testis is the commonest site to be affected, and being a sanctuary site for leukaemic infiltrates, testicular deposits may be the first manifestation of relapse. Like elsewhere, myeloid deposits may be either diffusely infiltrating or circumscribed masses resulting in testicular enlargement (Figure 16). Ancillary features include involvement of the epididymis and hydrocele.[5,7,11]

Retroperitoneum

Retroperitoneal chloroma stems from prevertebral/paraspinal deposits continuous with vertebral marrow infiltration or from involvement of lymph nodes. For its frequent asymptomatic occurrence, retroperitoneal masses tend to be large at presentation.

These deposits are either poorly marginated conglomerate lobulated masses (Figure 17) encasing the kidneys or ureters with variable infiltration into the paraspinal muscles or extension to the

Figure 17. A 45-year-old female, a known case of Chronic Myeloid Leukemia with blast crisis, presented with abdominal pain and weight loss. Contrast-enhanced CT revealed (a) hypovascular para-aortic mass (arrow). (b, c) Another distinct hypovascular mass was present at the pancreatic tail (arrows) which was infiltrating the splenic hilum with contiguous extension within the splenic parenchyma.

Figure 18. Musculoskeletal chloroma: (a) mixed lytic–sclerotic involvement of the pelvic bones, (b, c) axial and coronal contrast-enhanced CT (CECT) showing infiltrating enhancing mass involving the right glutei (straight arrows) and causing erosion of the ipsilateral iliac bone (curved arrows). (d) CECT taken 1 month post-chemotherapy showed significant reduction in size of the lesion. (e) Diffuse leukaemic marrow infiltration with lytic lesion in the lower cervical vertebra (arrow).

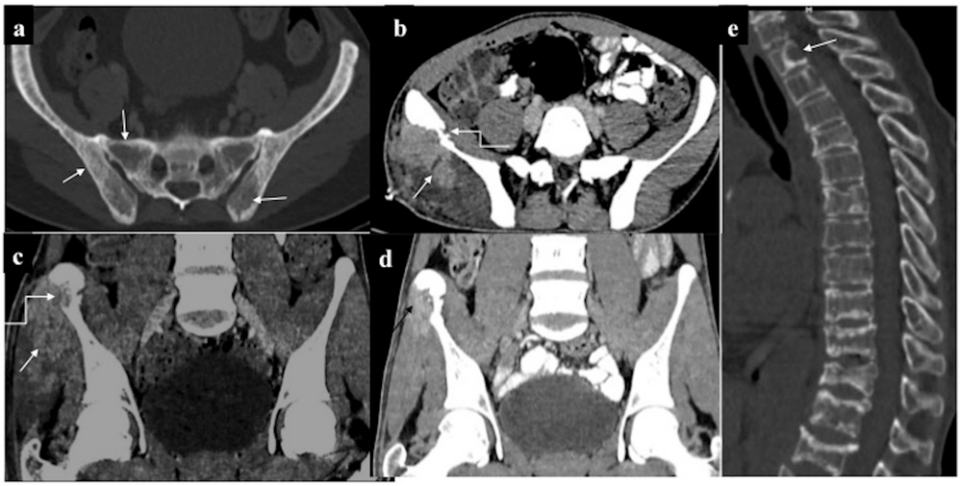

neural foramina. Less commonly, chloroma may deposit as plaque-like soft tissue which is indistinguishable from the retroperitoneal fibrosis on imaging. As elsewhere, retroperitoneal masses resemble lymphoma on imaging but the presence of compressive symptoms with leukaemic background suggests its diagnosis.[5,11]

Musculoskeletal system

Bone

The bone is the commonest site of extramedullary deposits particularly during leukaemic relapse. The axial skeleton is preferentially involved due to the persistence of haematopoietic marrow. In the appendicular skeleton, there is predilection for

Figure 19. Musculoskeletal chloroma: (a, b) contrast-enhanced CT of the pelvis of a leukaemic patient revealed ill-defined isodense soft tissue in the right hemipelvis (arrow) infiltrating the iliopsoas and piriformis muscles. Furthermore, it was infiltrating the mesorectal fascia with rectal involvement (curved arrow). Additionally, there was mild expansion and cortical thickening of the right iliac bone. (c, d) A different case with lytic expansile lesion with cortical thinning involving the ramus of the right hemimandible: biopsy revealed chloroma. 8 months post-chemotherapy, lesion had become sclerotic with no soft tissue component. (e) Another patient showing predominantly sclerotic involvement of the left hemimandible.

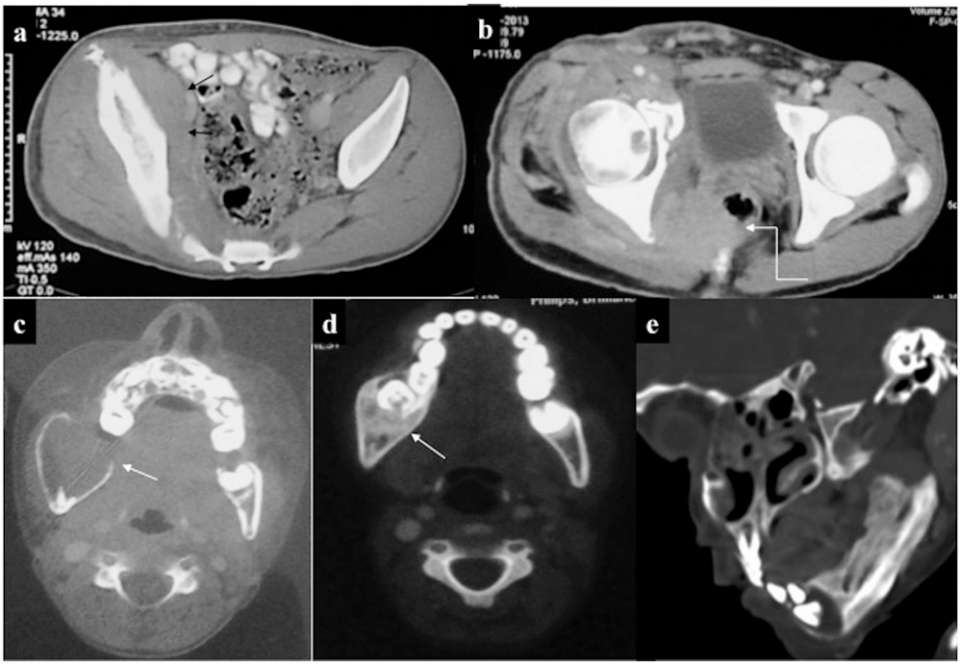

Figure 20. (a, b) Breast chloroma: a 23-year-old female, a known case of leukaemia; contrast-enhanced CT showed multiple circumscribed enhancing masses (arrows) in the bilateral breasts. (c) Follow-up scan performed 2 months post-chemotherapy showed complete disappearance of these masses. (d, e) Leukaemic lymphadenopathy: multiple large intensely enhancing left cervical lymphadenopathy (arrows). Additionally, infiltrating enhancing lesion at the base of the tongue involving soft palate was present (curved arrow in c). Another case (f) with bilateral enhancing axillary lymphadenopathy. (g) Ultrasonography of a different patient showing irregular hypoechoic deposit indistinguishable from carcinoma.

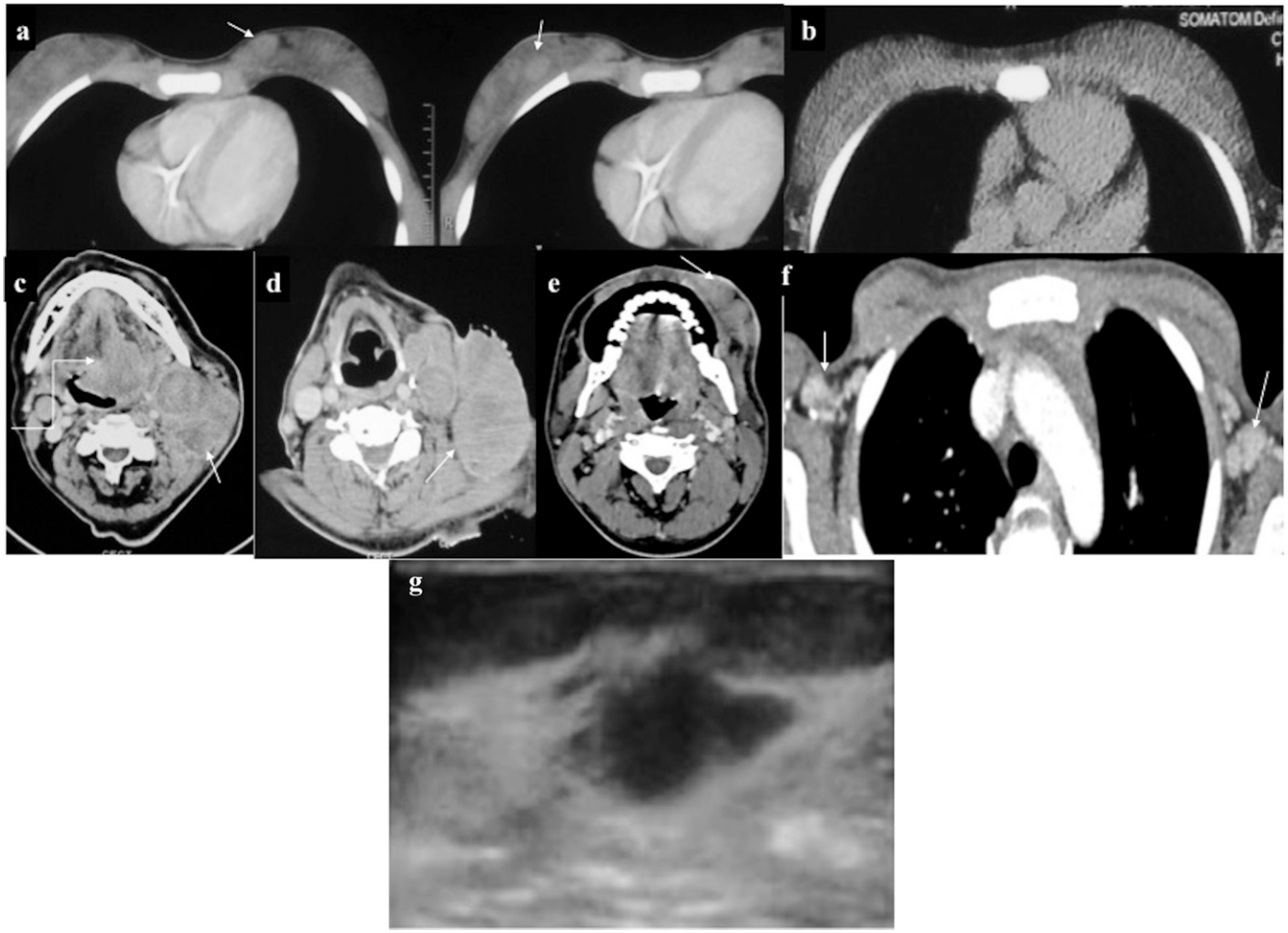

the involvement of the metadiaphyseal region. Radiographically, these lesions are commonly lytic with permeative bone destruction (Figure 18). Mixed-lytic sclerotic form has also been reported. There is proclivity for further ligamentous and periosteal spread consequent on the transgression of myeloid cells through the haversian canal. If unhalted, there may be infiltration into the surrounding muscles. MRI findings are non-specific; lesion is usually hypo-/isointense on T_1 and mildly hyperintense on T2WI with intense enhancement. Diagnostic certainty rises if it is isointense on both T_1 and T_2, making imaging distinction possible from other common bone lesions such as lymphoma, bone tumours or osteomyelitis which have higher signal intensity on T2WI.[5,7,29]

Muscle

Muscle deposits may be either primary or secondary to the involvement of the adjacent bone. Myeloid cells diffusely infiltrate the muscle causing enlargement. Of the various muscle groups, pelvic muscles are the most frequently affected. These deposits are isodense to the adjacent muscle on NCCT and show intense enhancement (Figure 19). There may be involvement of adjacent bone causing cortical erosion. On MRI, these lesions are isointense on T_1 and mildly T_2 hyperintense with intense enhancement.[5,7]

Subcutaneous tissue

Skin

Skin chloroma also called "leukaemia cutis" is fairly common, with reported incidence of 20–50%. It usually manifests as firm papulonodular lesions which may be solitary or multiple. These lesions may be painful and hence mistaken for abscesses or fat necrosis, especially in the background of immunosuppression.[5,7]

Table 2. Differential diagnosis of chloroma on imaging

Site	Imaging appearance of chloroma	Differential diagnosis	Distinguishing feature to suggest chloroma
(1) (a) Intracranial (extra-axial)	Hyperdense mass on NCCT MRI: T_1-hypo/isointense T_2-isointense/mildly hyperintense Marked and intense contrast enhancement	Lymphoma Meningioma Metastasis (neuroblastoma, Ewing's Sarcoma) Haematoma	–Usually bone destruction not a feature –Absence of bony hyperostosis and calcification, usually lack dural tail (c.f. meningioma) –High propensity for superficial venous sinus infiltration –Presence of enhancement (c.f. haematoma)
(b) Leptomeningeal involvement	Patchy or continuous meningeal enhancement	Non-neoplastic: infective, sarcoid Neoplastic: primary meningeal infiltration by lymphoma and metastasis	–Meningeal infiltration usually contiguous with dural forms –Leptomenigeal thickening may be hyperdense on NCCT
(2) Spine	Marrow infiltration with multiple extramedullary masses which are T_1-isointense T_2–intermediate signal intensity Homogeneous enhancement	Lymphoma Multiple myeloma EMH Metastasis nerve sheath tumour	–Lack of demonstrable fat (c.f. extra medullary haematopoiesis) –Intermediate T_2 signal intensity (c.f. T_2 hyperintensity in nerve sheath tumour)
(3) Orbit	Enhancing soft-tissue masses, may affect any orbital component MC site: subperiosteum	Haemangioma/lymphovenous malformation Rhabdomyosarcoma Ewing's sarcoma Lymphoma Neuroblastoma	Moulds along the confines of bony orbit, bone destruction usually lacking
(4) Hepatobiliary	Hypovascular nodules (solitary/multiple) Peribiliary chloroma	Lymphoma Abscess (cholangitis) Granulomatous disease (tuberculosis, sarcoid)	Compressive symptoms present (c.f. lymphoma)
(5) Gastrointestinal	Bowel involvement may be nodular, polypoidal, diffuse thickening Ancillary features: Lymphadenopathy, peritoneal and omental deposits, ascites	Lymphoma Adenocarcinoma	May have bowel obstruction (c.f. lymphoma)
(6) Skeletal	Lytic Mixed lytic-sclerotic	Lymphoma Histiocytic disorders Metastasis (neuroblastoma) Multiple myeloma/plasmacytoma Osteomyelitis	–
(7) Muscle	Isodense/isointense to muscle Homogeneous enhancement	Haematoma, myositis, focal nodular myositis, lymphoma	Homogeneous enhancement (c.f. hematoma, abscess)

c.f., refer; EMH, extramedullary haematopoiesis; MC, most common; NCCT, non-contrast CT.

Breast

Breast chloroma, although unusual, is relatively common in adult females. Lesions may be solitary or multiple with involvement of single or bilateral breasts (Figure 20). These masses lack calcification and may have either circumscribed or more frequently spiculated margins, making them indistinguishable from carcinoma on imaging. On ultrasound, it is hypoechoic and intensely enhancing on CECT or CEMRI. Imaging findings are indistinguishable from other breast malignancies such as carcinoma, lymphoma and metastasis[7–9]

Differential diagnosis

Few site-specific common differential considerations are enlisted (Table 2) which may mimic chloroma on imaging. These lesions have relatively common occurrence compared with chloroma and are frequently mistaken as second malignancy even in known cases of AML. Nevertheless, chloroma should always be suspected in masses with unusual imaging features (Figure 21). The key to correct interpretation is corroboration with clinical and Bone Marrow findings to accordingly direct the pathologist for diagnostic confirmation.

Figure 21. An algorithm for the management of chloroma. AML, acute myeloid leukaemia; BMT, Bone marrow transplantation; esp., Especially; MDS, myelodysplastic; MDS, myelodysplastic; MPL, myeloproliferative; MS, myeloid sarcoma; NCCT, non-contrast CT; RT, radiotherapy; T/t= treatment.

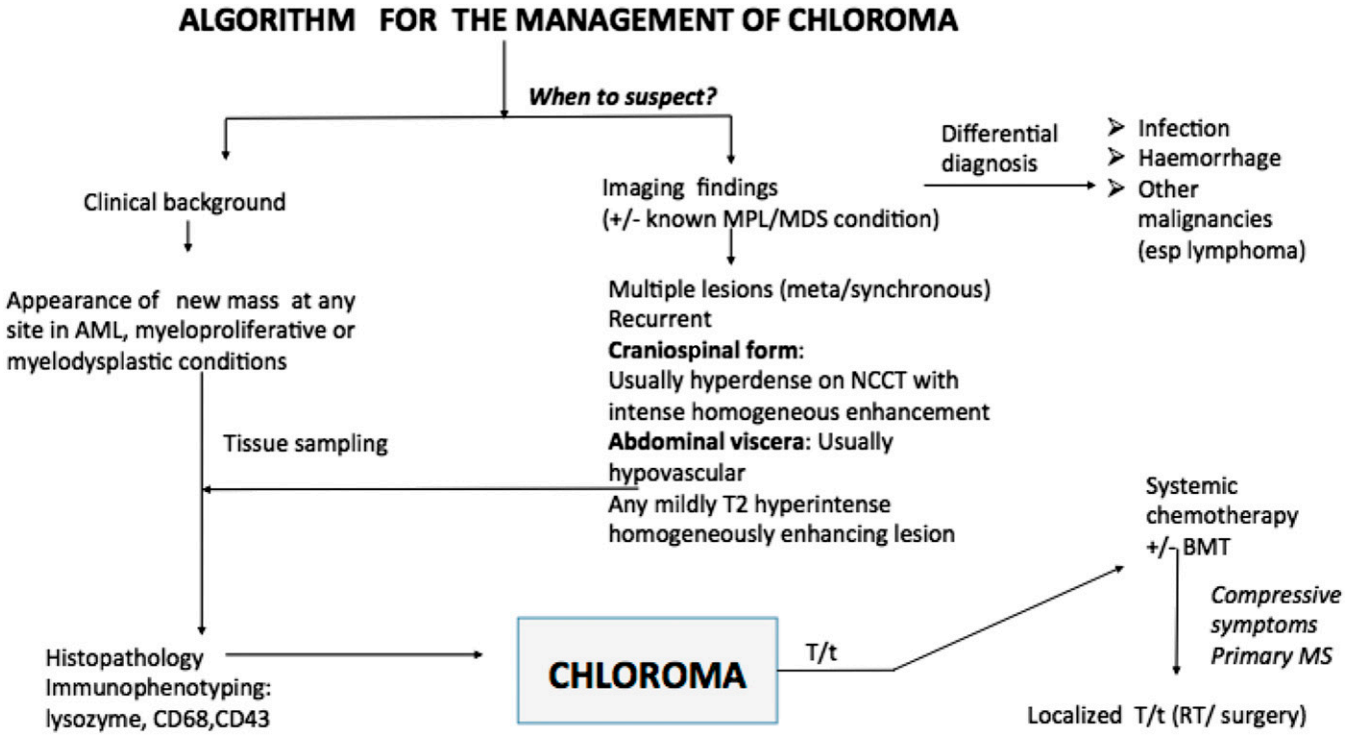

CONCLUSION

Chloroma, classically described in AML, may be seen in a horde of myeloproliferative or myelodysplastic conditions with non-specific clinical manifestations and imaging findings; diagnosing chloroma poses a challenge especially in the initial stages.

Exact prognostic implication of chloroma in AML remains uncertain, and the overall survival may remain unaffected; however, there may be increased refractoriness to treatment. Chloroma occurring in myeloproliferative/myelodysplastic conditions herald the onset of blast crisis, whereas primary myeloid sarcoma suggests an imminent leukaemic transformation. Irrespective of the site or Bone Marrow status, chloroma is treated by systemic chemotherapy. Localized treatment such as focused radiotherapy or surgery is performed at selected sites to relieve compressive symptoms. Radiologists play the central role in its management, hence familiarity with imaging features of chloroma is imperative to eye a suspicion for redirecting specific histopathological studies besides performing guided tissue sampling and obviating unnecessary surgery. Nonetheless, diagnosing chloroma is a holistic approach, taking into consideration the clinical background, imaging findings and eventual confirmation by IHC. Prompt and precise diagnosis is the key to successful management, as failure to institute treatment early leads to an inexorably aggressive downhill course with rapid mortality.

REFERENCES

1. Burns A. *Observations of surgical anatomy: head and neck*. Edinburgh, UK: Thomas Royce and Company; 1811. pp. 364–6.
2. King A. Case of chloroma. *Mon J Med Sci* 1853; **7**: 97.
3. Rappaport H. Atlas of tumor pathology. Sec. III, Fasicle 8, Washington, DC: Armed Forces Institute of Pathology.
4. Wilson CS, Medeiros LJ. Extramedullary manifestations of myeloid neoplasms. *Am J Clin Pathol* 2015; **144**: 219–39. doi: https://doi.org/10.1309/ajcpo58ywibubesx
5. Guermazi A, Feger C, Rousselot P, Merad M, Benchaib N, Bourrier P, et al. Granulocytic sarcoma (chloroma): imaging findings in adults and children. *AJR Am J Roentgenol* 2002; **178**: 319–25. doi: https://doi.org/10.2214/ajr.178.2.1780319
6. Lengerke C, Wirths S, Kanz L. Unusual leukemia presentations. *J Clin Oncol* 2005; **23**: 5837–9. doi: https://doi.org/10.1200/jco.2005.07.005
7. Fritz J, Vogel W, Bares R, Horger M. Radiologic spectrum of extramedullary relapse of myelogenous leukemia in adults. *AJR Am J Roentgenol* 2007; **189**: 209–18. doi: https://doi.org/10.2214/ajr.06.1500
8. Yilmaz AF, Saydam G, Sahin F, Baran Y. Granulocytic sarcoma: a systematic review. *Am J Blood Res* 2013; **3**: 265–70.
9. Audouin J, Comperat E, Le Tourneau A, Camilleri-Broët S, Adida C, Molina T, et al. Myeloid sarcoma: clinical and morphologic criteria useful for diagnosis. *Int J Surg Pathol* 2003; **11**: 271–82. doi: https://doi.org/10.1177/106689690301100404
10. Shinagare AB, Krajewski KM, Hornick JL, Zukotynski K, Kurra V, Jagannathan JP, et al.

MRI for evaluation of myeloid sarcoma in adults: a single-institution 10-year experience. *AJR Am J Roentgenol* 2012; **199**: 1193–8. doi: https://doi.org/10.2214/ajr.12.9057

11. Ooi GC, Chim CS, Khong PL, Au WY, Lie AK, Tsang KW, et al. Radiologic manifestations of granulocytic sarcoma in adult leukemia. *AJR Am J Roentgenol* 2001; **176**: 1427–31. doi: https://doi.org/10.2214/ajr.176.6.1761427
12. Bisschop MM, Révész T, Bierings M, van Weerden JF, van Wering ER, Hählen K, et al. Extramedullary infiltrates at diagnosis have no prognostic significance in children with acute myeloid leukaemia. *Leukemia* 2001; **15**: 46–9. doi: https://doi.org/10.1038/sj.leu.2401971
13. Cheng CL, Li CC, Hou HA, Fang WQ, Chang CH, Lin CT, et al. Risk factors and clinical outcomes of acute myeloid leukaemia with central nervous system involvement in adults. *BMC Cancer* 2015; **15**: 344. doi: https://doi.org/10.1186/s12885-015-1376-9
14. Kobayashi R, Tawa A, Hanada R, Horibe K, Tsuchida M, Tsukimoto I. Extramedullary infiltration at diagnosis and prognosis in children with acute myelogenous leukemia. *Pediatr Blood Cancer* 2007; **48**: 393–8. doi: https://doi.org/10.1002/pbc.20824
15. Pomeranz SJ, Hawkins HH, Towbin R, Lisberg WN, Clark RA. Granulocytic sarcoma (chloroma): CT manifestations. *Radiology* 1985; **155**: 167–70. doi: https://doi.org/10.1148/radiology.155.1.3856292
16. Ginsberg LE, Leeds NE. Neuroradiology of leukemia. *Am J Roentgenol* 1995; **165**: 525–34. doi: https://doi.org/10.2214/ajr.165.3.7645463
17. Algharras AA, Mamourian A, Coyne T, Mohan S. Leukostasis in an adult with AML presenting as multiple high attenuation brain masses on CT. *J Clin Diagn Res* 2013; **7**: 3020–2. doi: https://doi.org/10.7860/JCDR/2013/6638.3893
18. Vázquez E, Lucaya J, Castellote A. Neuroimaging in pediatric leukemia and lymphoma: differential diagnosis. *Radiographics* 2002; **22**: 1411–28. doi: https://doi.org/10.1148/rg.226025029
19. Parker K, Hardjasudarma M, Mcclellan RL, Fowler MR, Milner JW. MR features of an intracerebellar chloroma. *AJNR Am J Neuroradiol* 1996; **17**: 1592–4.
20. Smidt MH, De bruin HG, van Veer MB, van den Bent MJ. Intracranial granulocytic sarcoma (chloroma) may mimic a subdural hematoma. *J Neurol* 2005; **252**: 498–9. doi: https://doi.org/10.1007/s00415-005-0680-8
21. Mallory GM, Van Gompel JJ, Rabinstein AA, Fugate JE, Lanzino G. Wolf in sheep's clothing: acute chloroma disguised as a subdural hematoma. *Neurocrit Care* 2012; **16**: 148–50. doi: https://doi.org/10.1007/s12028-011-9631-7
22. Freedy RM, Miller KD. Granulocytic sarcoma (chloroma): sphenoidal sinus and paraspinal involvement as evaluated by CT and MR. *AJNR Am J Neuroradiol* 1991; **12**: 259–62.
23. Seok JH, Park J, Kim SK, Choi JE, Kim CC. Granulocytic sarcoma of the spine: MRI and clinical review. *AJR Am J Roentgenol* 2010; **194**: 485–9. doi: https://doi.org/10.2214/ajr.09.3086
24. Anqi X, Siqing H, Zhenlin L, Chao Y. Sacral canal myeloid sarcoma as initial manifestation of granulocytic leukemia: MRI features and differential diagnosis (with a case report). *Turk Neurosurg* 2014; **24**: 281–3. doi: https://doi.org/10.5137/1019-5149.JTN.7125-12.1
25. Noh BW, Park SW, Chun JE, Kim JH, Kim HJ, Lim MK. Granulocytic sarcoma in the head and neck: CT and MR imaging findings. *Clin Exp Otorhinolaryngol* 2009; **2**: 66–71. doi: https://doi.org/10.3342/ceo.2009.2.2.66
26. Zimmerman LE, Font RL. Ophthalmic manifestations of granulocytic sarcoma (myeloid sarcoma or chloroma). *Am J Ophthalmol* 1975; **80**: 975–90. doi: https://doi.org/10.1016/0002-9394(75)90326-8
27. Kovalski R, Hansen-Flaschen J, Lodato RF, Pietra GG. Localized leukemic pulmonary infiltrates. Diagnosis by bronchoscopy and resolution with therapy. *Chest* 1990; **97**: 674–8. doi: https://doi.org/10.1378/chest.97.3.674
28. Prayongratana K, Kulpraneet M, Panichchob P, Tantisiriwat W. Acute monoblastic leukemia with t(10;11)(p12;q23) presenting with pulmonary involvement: a case report and literature review. *J Med Assoc Thai* 2008; **91**: 559–63.
29. Hermann G, Feldman F, Abdelwahab IF, Klein MJ. Skeletal manifestations of granulocytic sarcoma (chloroma). *Skeletal Radiol* 1991; **20**: 509–12.